Applied Catalysis B: Environmental 94 (2010) 55–63

Contents lists available at ScienceDirect

Applied Catalysis B: Environmental

journal homepage: www.elsevier.com/locate/apcatb

Dechlorination of chloroacetic acids by Pd/Fe nanoparticles: Effect of drying method on metallic activity and the parameter optimization

Xiangyu Wang [a,b], Ping Ning [b], Huiling Liu [a,*], Jun Ma [a]

[a] School of Municipal and Environmental Engineering, State Key Laboratory of Urban Water Resources and Environment, Harbin Institute of Technology, Haihe Road 202#, Nangang District, Harbin 150090, China
[b] Department of Environmental Science and Engineering, Kunming University of Science and Technology, Kunming 650093, China

ARTICLE INFO

Article history:
Received 25 February 2009
Received in revised form 18 October 2009
Accepted 26 October 2009
Available online 5 November 2009

Keywords:
Pd/Fe nanoparticles
Drying method
Chloroacetic acid
Catalytic dechlorination
Metallic activity

ABSTRACT

Two kinds of dry Pd/Fe nanoparticles (Pd/Fe-1 and Pd/Fe-2) were obtained by drying the laboratory synthesized wet Pd/Fe nanoparticles with direct oven drying method and solvent replacement oven drying method, respectively. A comparison was made between the two drying methods, concerning the effects of the washing reagents used during the drying process on the physicochemical properties and the activities of Pd/Fe nanoparticles for catalytic dechlorination of chloroacetic acids. Pd/Fe nanoparticles prepared by impregnation of iron nanoparticles with an aqueous solution of potassium hexachloropalladate were washed with different reagents (deionized water and organic solvents), followed by vacuum drying in an oven at 100 °C. The prepared dry Pd/Fe-1 and Pd/Fe-2 nanoparticles were characterized in terms of specific surface area (BET-N_2), morphology (SEM), surface elemental distribution (EDS), and particle size (TEM). The catalytic activities of Pd/Fe-1 and Pd/Fe-2 nanoparticles were evaluated via dechlorination reaction of chloroacetic acids including trichloroacetic acid (TCAA), dichloroacetic acid (DCAA), and monochloroacetic acid (MCAA). The removal efficiencies of chloroacetic acids by Pd/Fe-2 were about 58.5–22.7% greater than that achieved by Pd/Fe-1. The optimal Pd content, the amount of metal loading, and the initial pH value of reaction system for higher removal efficiency of chloroacetic acids were determined. The variation of pH value, dechlorination pathway and kinetics of chloroacetic acids were also investigated. The removal efficiencies of chloroacetic acids followed the order of TCAA > DCAA > MCAA with observed reaction rate constant (k_{obs}) values of 1.113×10^{-1}, 1.278×10^{-2}, and 1.900×10^{-3} min^{-1}, respectively.

1. Introduction

Chloroacetic acids, including trichloroacetic acid (TCAA), dichloroacetic acid (DCAA), and monochloroacetic acid (MCAA) are commonly detected contaminants in aqueous environment formed via the chlorination of drinking water or wastewater due to the reaction of chlorine with organic compounds in water. TCAA, DCAA and MCAA are three important disinfection by-products (DBPs), and proved to be carcinogenic and potentially of great risk to human health [1,2]. In the United States, the maximum contaminant level of the sum of the concentrations of TCAA, DCAA, MCAA, monobromoacetic acid (MBAA), and dibromoacetic acidic (DBAA) is proposed to be 60 μg/L [3]. The safety levels for DCAA and TCAA recommended by the World Health Organization are 50 and 100 μg/L, respectively. The degradation of chloroacetic acids in aqueous phase is receiving growing concern.

Zero-valent iron (ZVI) technology is a promising treatment for degradation of halogenated organic compounds (HOCs) and has been intensively investigated in the last decades [4,5]. As a strong reductant, ZVI can degrade a wide range of HOCs. The overall dechlorination reaction process of HOC by ZVI is shown as follows:

$$Fe^0 + RX + H^+ \rightarrow Fe^{2+} + RH + X^- \quad (1)$$

where RX is a generalized halogenated hydrocarbon. The use of Pd amended iron nanoparticles for catalytic dechlorination of HOCs has received much attention due to the significant enhancement in both removal efficiency and reaction rate. The transition metal Pd plays two key roles in dechlorination reaction: (1) dissociatively chemisorbing H_2 generated from the iron corrosion [6,7] and (2) decomposing H_2 into atomic H*, a highly activated intermediate hydrogen radical [8].

Several studies exist regarding the degradation of haloacetic acids (HAAs) with zero-valent iron. Hozalski et al. [9] and Zhang

* Corresponding author.
E-mail address: wxy_hit2007@126.com (H. Liu).

0926-3373/$ – see front matter © 2009 Elsevier B.V. All rights reserved.
doi:10.1016/j.apcatb.2009.10.020

et al. [10] investigated the reduction of HAAs by Fe^0, their results proved that four trihaloacetic acids, trichloroacetic acid (TCAA), tribromoacetic acid (TBAA), chlorodibromoacetic acid (CDBAA), and bromodichloroacetic acid (BDCAA), reacted rapidly with Fe^0, but other HAAs, such as MCAA, were found to be relatively persistent in dechlorination reaction with iron, and the removal of these HAAs remains a difficult challenge. Iron-based bimetallic particles (e.g. Pd/Fe, Ni/Fe, Cu/Fe) were used to enhance the removal efficiency of some recalcitrant HOCs [11]. We are unaware of any studies in the literature on catalytic dechlorination of chloroacetic acids by Pd/Fe nanoparticles. For practical application, determining the optimal dechlorination conditions of chloroacetic acids with Pd/Fe nanoparticles are of particular importance. ZVI nanoparticles or iron-based bimetal nanoparticles, such as Pd/Fe, Ag/Fe, Ni/Fe, Cu/Fe are not yet commercially available, and have to be synthesized in laboratory for treatment of HOCs. In general, the methods for preparation of nanoparticles can be classified into three categories according to the state of the reactant: gas phase method, liquid phase method, and solid phase method. By far, the liquid phase method is the most popular method for preparation of ZVI nanoparticles in both laboratory and industry [12]. ZVI nanoparticles were post-coated with Pd using the electro-chemical method. At least two distinct synthetic schemes are commonly adopted for preparation of Pd/Fe bimetallic nanoparticles: (1) palladizing iron nanoparticles in an ethanol solution of palladium acetate and (2) palladizing iron nanoparticles in an aqueous solution of potassium hexachloropalladate. Despite the intensive study of dechlorination of HOCs by ZVI or iron-based bimetal over the last decade, there are still some challenges to apply the ZVI technology. From a fundamental research point of view, Pd/Fe nanoparticles are utilized in laboratory either in wet state or in dry state for the investigation of dechlorination efficiency of HOCs. But taking into account potentially wide applications, the use of wet metallic nanoparticles for in situ remediation of HOCs brings extreme inconvenience. As one of the storage method, nanoparticles can be kept in proper solution to prevent their deactivation. However, it is more advantageous to transport nanoparticles in dry state than to transport nanoparticles stored in aqueous solution. The exposure of the wet Pd/Fe nanoparticles to air results in immediate oxidation of the particles. In addition, nanoparticles can be deactivated if they are stored with improper method. Currently, no widely accepted storage method for satisfactory preservation of wet Pd/Fe nanoparticles has been established. On the other hand, the utilization of Pd/Fe in dry state provides enormous flexibility either in situ or ex situ remediation application. Therefore, the dechlorination of HOCs by Pd/Fe nanoparticles with high activity in dry state can be considered as a promising means of contaminant remediation. Besides, nanoparticles must be in dry state for accurate identification of their characteristics (e.g. morphology, surface area, particle shape and size, and crystal structure) and precise determination of their important parameter (e.g. metal loading, elemental composition) in dechlorination reaction. On all accounts, developing a drying method capable of obtaining Pd/Fe nanoparticles in dry state without destroying their physiochemical properties and deactivating their catalytic activity is a challenging task. As for nanoparticles prepared by liquid phase method, drying process of wet particles is a crucial operation, because nanoparticles tend to aggregate and their physical and/or chemical properties can be adversely affected if inappropriate drying methods are chosen [13]. In respect that both the reactivity and degradation efficacy of nanoparticles in contaminant remediation could be significantly affected by the aggregation behavior of nanoparticles, an insightful understanding of the aggregation behavior under different condition is urgently needed [14]. At this point, the establishment of an effective drying method for the preparation of nanoparticles in dry state with high activity is extremely worthwhile for environmental applications.

In our previous study, wet Pd/Fe nanoparticles palladized by an ethanol solution of potassium hexachloropalladate were successfully dried by vacuum-drying method, and the harvested dry Pd/Fe nanoparticles showed high dechlorination activity [15]. So far, to the best of our knowledge, wet Pd/Fe nanoparticles prepared by using an aqueous solution of potassium hexachloropalladate as palladizing solution were added immediately for catalytic dechlorination of HOCs [16–18]. For instance, Morales et al. synthesized palladized iron powder by adding iron powder (100 mesh) in an aqueous solution of potassium hexachloropalladate, followed by its immediate use for in situ dechlorination of chlorinated phenols [19]. They further reported that their attempts to store palladized iron powder for long-term preservation failed due to the rapid oxidation of the bimetallic particle surface caused by the galvanic corrosion characteristics of iron. In general, the studies involving dechlorination of HOCs by the Pd/Fe nanoparticles that were palladized by using potassium hexachloropalladate did not report any details related to the effect of drying method on physiochemical properties and the activity of Pd/Fe nanoparticles in dry state. Little effort has been made to obtain dry Pd/Fe nanoparticles prepared by using the aforementioned approach for dechlorination of HOCs.

The primary objective of this study is to develop a practically effective method for drying Pd/Fe nanoparticles palladized by an aqueous solution of potassium hexachloropalladate. Furthermore, the specific objectives of this study include: (1) identifying the intermediates and final products of catalytic dechlorination of chloroacetic acids, (2) determining the dechlorination rate of chloroacetic acids by dry Pd/Fe nanoparticles, and (3) proposing the possible catalytic dechlorination pathway of chloroacetic acids by Pd/Fe nanoparticles. In this study, synthetic scheme of Pd/Fe nanoparticles involved the reduction of iron from aqueous solution of ferrous sulfate using potassium borohydride as the reductant and the palladization of ZVI using potassium hexachloropalladate. Wet Pd/Fe nanoparticles were washed with deionized water and organic solvents (ethanol and acetone), respectively, followed by vacuum-dried in an oven without the protection of nitrogen. Characterization of Pd/Fe nanoparticles and batch experiments of dechlorination of chloroacetic acids were performed to investigate the effects of different drying methods on the physicochemical properties and dechlorination activity of Pd/Fe nanoparticles in dry state. The pH variation during the experiments was determined for investigating the plausible effects of pH change on the removal efficiency of chloroacetic acids.

2. Materials and methods

2.1. Chemicals

Potassium borohydride (KBH_4) (99.995%), ferrous sulfate ($FeSO_4{\cdot}7H_2O$, 99.8%), and ethanol were obtained from Kermel (Tianjin, China). Potassium hexachloropalladate (K_2PdCl_6, 99%) was purchased from Aldrich (Milwaukee, WI, USA). TCAA (Cl_3CCOOH), DCAA ($Cl_2CHCOOH$), MCAA ($ClCH_2COOH$), and acetic acid (CH_3COOH) were from Ourchem (Sinopharm Chemical Reagent Corp. Ltd.).

All chemicals used in this study were of analytical reagent grade and used without further purification.

2.2. Preparation of Pd/Fe nanoparticles

Two commonly adopted routes are presently employed to prepare ZVI nanoparticles by using ferric chloride hexahydrate and ferrous sulfate heptahydrate as the principal ZVI precursor salts,

respectively. As pointed out by Zhang et al., ferrous sulfate method is more advantageous than the ferric chloride method for several reasons: (1) ferric chloride is a highly acidic salt with hygroscopy, (2) preparation of ZVI nanoparticles from ferric as starting cation requires more borohydride than that from ferrous as starting cation, and (3) excessive chloride from experiment may bring negative effect on dechlorination reactions [20]. Therefore, $FeSO_4$ was chosen as precursor for the preparation of ZVI nanoparticles in this study. An aqueous 0.5 mol/L KBH_4 solution was added dropwise to equal volume of aqueous 0.28 mol/L $FeSO_4$ solution in an anaerobic glovebox under a N_2 atmosphere to prevent the oxidation of freshly prepared ZVI. KBH_4 added was excessive according to stoichiometric requirement (Eq. (2)) in order to ensure complete reduction of ferrous ions:

$$Fe^{2+} + 2BH_4^- + 6H_2O \rightarrow Fe^0 \downarrow + 2B(OH)_3 + 7H_2 \uparrow \quad (2)$$

The ZVI nanoparticles were rinsed with a large excess of deionized water and harvested through vacuum-filtration. Pd/Fe nanoparticles were prepared by wet impregnation of iron nanoparticles into 0.4 g/L potassium hexachloropalladate solution, resulting in the spontaneous deposition of Pd on iron surface via redox reaction (Eq. (3)):

$$PdCl_6^{2-} + 2Fe^0 \rightarrow 2Fe^{2+} + Pd^0 \downarrow + 6Cl^- \quad (3)$$

The palladizing process was completed till deep orange potassium hexachloropalladate solution turned to a pale yellow solution. To compare the effect of washing reagents and drying procedure on the catalytic activity of Pd/Fe nanoparticles, the freshly prepared Pd/Fe nanoparticles were divided into two equivalent portions, and post-treated with two different drying methods:

(1) *Direct oven drying method*. The wet Pd/Fe nanoparticles were washed and filtered with excess amount of deionized water, and then the harvested particles were vacuum-dried in an oven at 100 °C for 6 h, followed by naturally cooled to room temperature. The dry Pd/Fe nanoparticles obtained by direct oven drying method are referred to as Pd/Fe-1 throughout the presentation.
(2) *Solvent replacement oven drying method*. The wet Pd/Fe nanoparticles were washed with a large amount of deionized water, rinsed with ethanol, filtered with acetone, vacuum-dried in an oven at 100 °C for 6 h, and then gradually cooled to room temperature. The dry Pd/Fe nanoparticles obtained by solvent replacement oven drying method are referred to as Pd/Fe-2 in this study.

The dry Pd/Fe nanoparticles were ground using an agate mortar and pestle in an anaerobic glovebox to break up the loosely attached aggregates and acquire fine grains, and then stored in vials for characterization and dechlorination reaction.

2.3. Physical characterization of Pd/Fe nanoparticles

BET (Brunauer–Emmett–Teller) surface area of Pd/Fe nanoparticles was measured with an Autosorb-1 surface analyzer (Quantachrome Corp., Boynton Beach, FL, USA) by employing nitrogen adsorption method. The morphology of Pd/Fe nanoparticles was observed by a MX2600FE scanning electron microscope (SEM, Camscan Ltd., UK). The surface elemental compositions of Pd/Fe nanoparticles were identified through an energy dispersive X-ray spectrometer (EDS, Oxford Instrument, UK) in conjunction with SEM. The size of Pd/Fe nanoparticles was measured using a 100 keV Hitachi H 7650 transmission electron microscope (TEM). Dry Pd/Fe nanoparticles were put into acetone solution and ultrasonicated for 5 min. Next, several droplets of the Pd/Fe nanoparticle/acetone suspension were deposited on a 300-mesh Cu-grid, followed by the evaporation of acetone.

2.4. Dechlorination of chloroacetic acids by dry Pd/Fe nanoparticles

A series of glass vials were filled with 50 mL of an aqueous solution of chloroacetic acid allowing for about a 10-mL headspace. A desired amount of Pd/Fe nanoparticles was loaded into the vials. The vials were sealed with Telfon-lined rubber septa and aluminum cap immediately, and then placed on an orbital shaker and agitated at 170 rpm at room temperature (22 ± 1 °C) throughout the duration of the dechlorination experiment. At selected time intervals, duplicate sample vials were sacrificed and liquid samples were taken with a gas-tight syringe and then filtered through a 0.22-μm Millipore syringe filter for subsequent analyses. All experiments were performed in triplicate.

2.5. Analytical methods

For analyses of chloroacetic acids, TCAA, DCAA, and MCAA were methyl esterified and analyzed using an HP 4890 GC equipped with an HP-5 capillary column (30 m long, 0.32 mm internal diameter, 0.25 μm thickness) and an electron capture detector (ECD). The flow rate of ultra-high-purity nitrogen carrier gas was 60 mL/min. The samples were injected with a volume of 1.0 μL using a 0.1 mL glass syringe. The oven temperature program used was 5 min at 40 °C, with a temperature ramp of 20 °C/min up to 140 °C, 10 °C/min to 160 °C, 25 °C/min to 240 °C, and 3 min at 240 °C. The injector port and detector temperatures were set at 220 and 300 °C, respectively.

Acetic acid was analyzed using an HP 6890 GC equipped with an Inwax capillary column (30 m, 1.53 mm, 1.0 μm) and an FID. The samples were injected with a volume of 1.0 μL. The temperatures of injector and detector were fixed at 220 °C. The oven temperature condition was programmed as follows: initial oven temperature of 90 °C with hold time for 2 min, ramped at a rate of 35 °C/min to 170 °C with hold time for 25 min, and increased at a rate of 65 °C/min to final temperature of 230 °C:

$$\text{removal efficiency}\,(\%) = \left(1 - \frac{C}{C_0}\right) \times 100 \quad (4)$$

where C denotes the concentration of chloroacetic acid at time t and C_0 denotes the initial concentration of chloroacetic acid.

3. Results and discussion

3.1. Surface area, morphology, size, and elemental composition of Pd/Fe nanoparticles

The specific surface areas of Pd/Fe-1 and Pd/Fe-2 nanoparticles were measured to be 32.4 and 36.5 m^2/g, respectively. Fig. 1 shows the size difference between Pd/Fe-1 and Pd/Fe-2 nanoparticles. The diameters of Pd/Fe-1 and Pd/Fe-2 nanoparticles ranged generally from around 40 to 70 nm and 30 to 50 nm, respectively. Pd/Fe nanoparticles aggregated each other due to the magnetic effects between the smaller primary particles. Pd/Fe-1 nanoparticles were observed to aggregate more severely than Pd/Fe-2 nanoparticles. Most Pd/Fe-1 nanoparticles were irregular in size and shape, and on the contrary, Pd/Fe-2 nanoparticles were roughly spherical and evenly sized.

Fig. 2 shows the EDS patterns of Pd/Fe-1 and Pd/Fe-2 nanoparticles. For Pd/Fe-1, the characteristic peaks of element Fe, Pd, and O were identified, confirming the oxidation of Pd/Fe nanoparticles. It may be concluded that the surface of Pd/Fe-1 was largely present as iron hydroxides and/or iron oxides. The

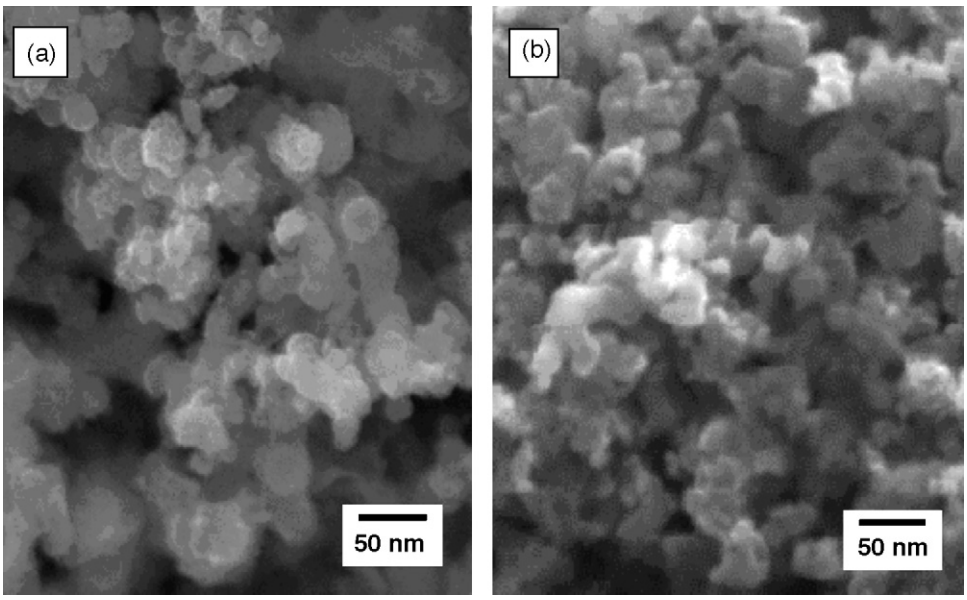

Fig. 1. SEM images of Pd/Fe nanoparticles: (a) Pd/Fe-1 and (b) Pd/Fe-2.

oxidation of ZVI nanoparticles might be due to the reaction between iron and the dissolved oxygen during the heating process. In the case of Pd/Fe-2, the characteristic peaks of Pd and Fe confirmed the bimetallic structure of Pd/Fe-2, while the O peak is neglectable, substantiating that Pd/Fe-2 nanoparticles have not been oxidized during the drying process.

As shown in Fig. 3, Pd/Fe-1 nanoparticles heavily aggregated each other. No single Pd/Fe nanoparticle is visually distinguishable from Fig. 3(a). This result was in good agreement with that shown in the SEM images (Fig. 1). Further more, it can also be expected that the severe aggregation of Pd/Fe-1 led to the reduction of its total surface area. Thereby, the measured surface area of Pd/Fe-1 is smaller than that of Pd/Fe-2. As shown in Fig. 3(b), Pd/Fe-2 particles are spherical beads, and they intertwined each other to form a chainlike structure. The typical Pd/Fe-2 particle size was around 30–40 nm. Whereas, the aggregation of Pd/Fe-1 particles made the precise measurement of their diameter difficult (Fig. 3(a)). The clusters of small particles on the surface of the sample indicated the presence of iron oxides. Approximately, most Pd/Fe-1 particle sizes were in the range of 40–80 nm.

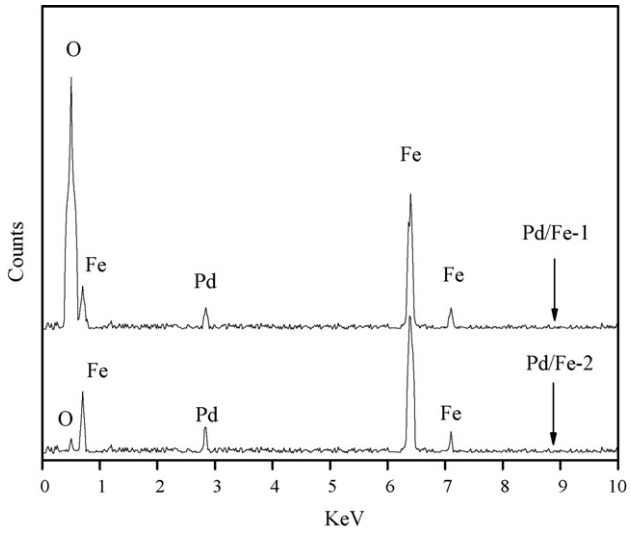

Fig. 2. EDS patterns of Pd/Fe nanoparticles.

3.2. Removal efficiency of chloroacetic acids by different dry Pd/Fe nanoparticles

Fig. 4 graphically presents that the removal efficiencies of chloroacetic acids with Pd/Fe-2 are greater than that with Pd/Fe-1. The oxidation and aggregation of Pd/Fe-1 nanoparticles were the crucial reasons that resulted in the relatively low activity for dechlorination of chloroacetic acids. During the drying process of wet Pd/Fe-1 nanoparticles, deionized water was used as washing reagent. As a consequence, Pd/Fe-1 nanoparticles could be easily oxidized mostly due to the presence of dissolved oxygen in water under vacuum drying at high temperature. In contrast, the oxidation of Pd/Fe-2 had not taken place because organic solvents were used as washing reagents during the drying process of Pd/Fe-2 nanoparticles.

Drying process is an essential step of nanoparticles prepared by the liquid phase method. Washing with water and filtration are indispensable steps for nanoparticles prepared by liquid phase method to get rid of the residual ions, but these two steps usually cause severe aggregation. The surface area of Pd/Fe nanoparticles decreased with the aggregation of particles, resulting in the loss of active sites and eventually the decrease in the dechlorination activity of Pd/Fe nanoparticles. The aggregation of nanoparticles is attributed to the van der waals force and/or the chemical bond between the particles. The aggregation that takes place due to the van der waals force is usually referred to as soft agglomeration, and can be prevented by using physical and chemical methods, such as stabilization of nanoparticles by attaching a stabilizer such as a soluble polymer or surfactant onto the nanoparticles [21]. While the aggregation of nanoparticles due to the chemical bond (hard agglomeration) during the drying process is more complicated, and cannot be prevented by simple physical method. The combined actions of the overplus surface energy of nanoparticles, the surface tension of liquid, and the interphase tension between nanoparticles and liquid contribute to the strong tendency of particles to aggregate [12]. The Pd/Fe bimetallic aggregates observed in SEM and TEM images were actually composed of nano-sized primary particles. The surface energy of nanoparticles is decreased and the nanoparticles tend to be more stable via aggregation. The effect of drying methods on the aggregation tendency of Pd/Fe nanoparticles is schematically depicted in Scheme 1. Because Pd/Fe-1 nanoparticles were washed with deionized water during the

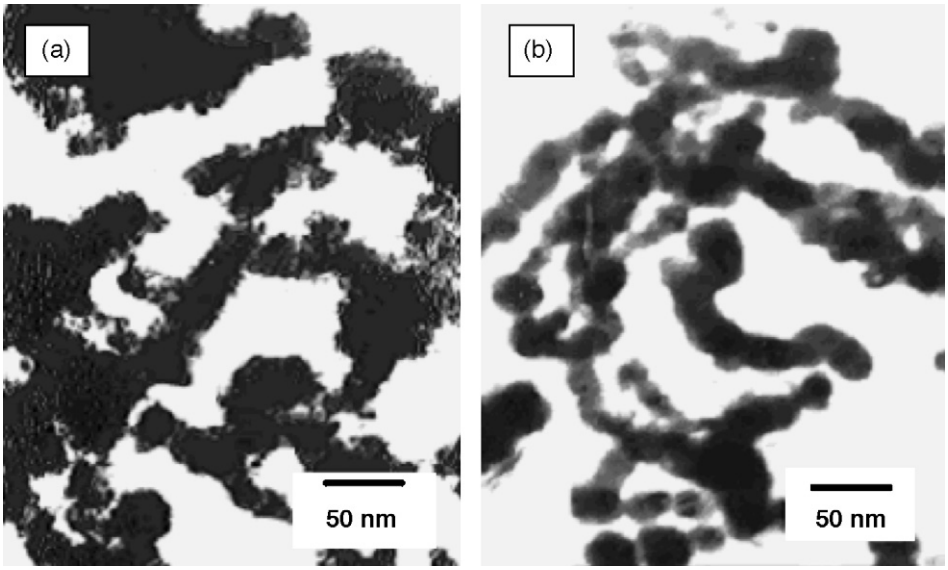

Fig. 3. TEM image of Pd/Fe nanoparticles: (a) Pd/Fe-1 and (b) Pd/Fe-2.

drying process, the non-bridge hydroxyl groups between neighboring nanoparticles were transformed into bridge hydroxyls (–O–), resulting in production of the more stable complex Fe–O–Fe (Scheme 1(a)). With the reducing of coordinated water, nanoparticles became closer and closer due to capillarity, more and more –O– were formed to account for the aggregation of Fe nanoparticles.

The aggregation due to the chemical bond can be prevented by either reducing the surface tension and capillary pressure between particles or reducing the interaction force by means of enlarging the distance between the nanoparticles. Washing the wet nanoparticles with organic solvent is an effective way to decrease the water content and reduce the surface tension of wet nanoparticles. Typically, the surface tensions of organic solvents, such as ethanol (γ = 0.0223 N m^{-1}), methanol (γ = 0.0224 N m^{-1}), and acetone (γ = 0.0240 N m^{-1}) are lower than that of water (γ = 0.0720 N m^{-1}). Scheme 1(b) shows the function of ethanol (Et–OH) when being used as washing reagent of wet nanoparticles. Water in nanoparticles was replaced by ethanol, as a result, the formation of bridge hydroxyl –O– was prevented, and meanwhile, the distance between nanoparticles was also enlarged due to sterically hindered effects. In order to further reduce the surface tension of Pd/F-2 nanoparticle and quicken the filtration process, acetone was used to wash wet particles as a supplementary organic solvent. Consequently, aggregation of Pd/Fe-2 nanoparticles was prevented by washing wet particles with organic solvents, and the activity of Pd/Fe-2 nanoparticles is greater than that of aggregated Pd/Fe-1 nanoparticles. Dry Pd/Fe-2 nanoparticles were used in the subsequent dechlorination experiments of this study.

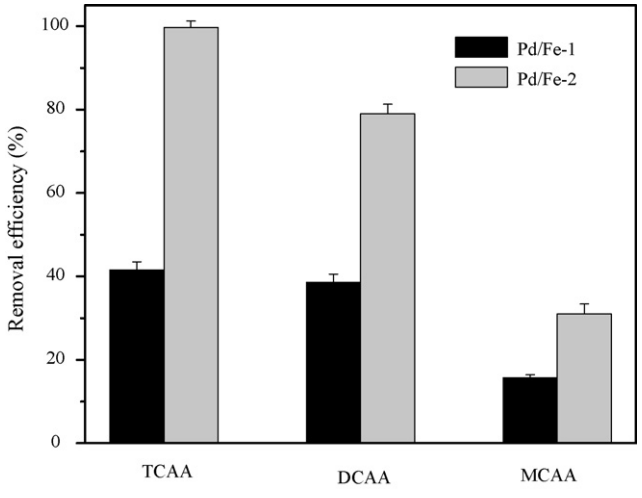

Fig. 4. Comparison of the removal efficiencies of chloroacetic acids by different Pd/Fe nanoparticles (Pd content = 0.1 wt%, Pd/Fe loading = 3 g/L, initial concentration of chloroacetic acid = 20 mg/L, and reaction time = 180 min). Values and the error bars represent the average and the standard deviation from the triplicate runs, respectively.

3.3. Effect of Pd content on the removal efficiency of chloroacetic acids

According to previously reported results, the dechlorination reaction rate of HOCs can be significantly increased by using ZVI nanoparticles post-coated with a small amount of Pd [4,17,18,22,23]. But taking into account that Pd is noble metal and the addition of Pd to water may cause environmental problems, it is of great importance to find the minimum Pd content that is still effective for catalytic dechlorination of chloroacetic acids. From Fig. 5, the removal efficiency was found to increase with increasing the Pd content, and maximized at 0.1 wt%. However, the removal efficiency decreased when the Pd content increased from 0.1 to 0.2 wt%. Bodnariuk et al. assumed that Pd and Cl could form a strong bond Pd–Cl [24]. Therefore, it can be supposed that a transitional compound Pd···Cl···R was formed on the surface of Pd/Fe nanoparticles during the dechlorination of chloroacetic acids. Furthermore, the amount of the transitional compound Pd···Cl···R on the surface of Pd/Fe nanoparticles increased with increasing the Pd content, resulting the increase of removal efficiency. When the Pd content exceeded 0.1 wt%, more hydrogen bubbles were accumulated on the surface of Pd/Fe nanoparticles. The extensive hydrogen gas formation resulted in the decrease of removal efficiency [25,26]. He et al. also demonstrated that at a Pd content of <0.1 wt%, the amount of Pd is the limiting factor affecting dechlorination rate while the iron corrosion or the formation of atomic H is the limiting factor for dechlorination of target pollutant TCE at a Pd content of >0.1 wt% [27]. As was also reported by Zhang et al., relatively lower Pd content was required in order to get optimal performance of the Pd/Fe nanoparticles. According to their research, no dechlorination reaction occurred when Pd content was greater than 50 wt% [28].

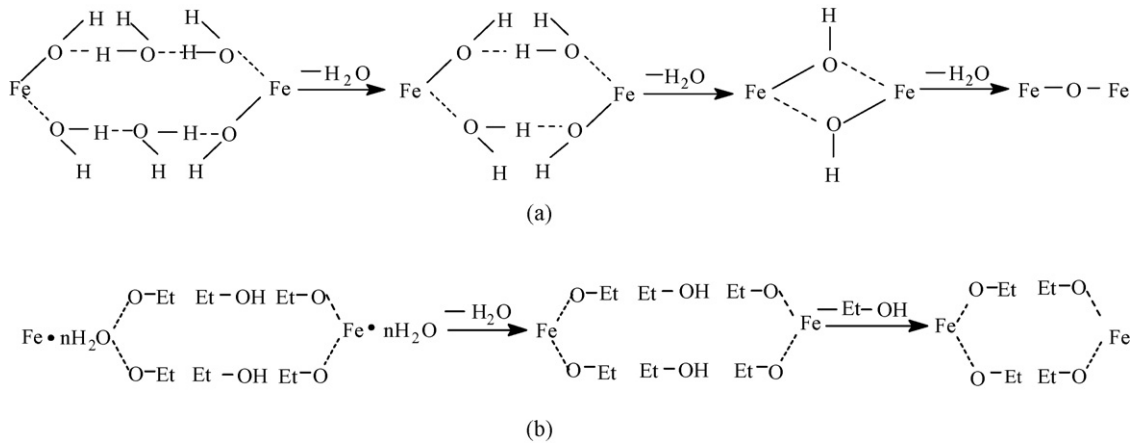

Scheme 1. Drying process of wet Pd/Fe nanoparticles using different methods: (a) direct oven drying method and (b) solvent replacement oven drying method.

3.4. Effect of Pd/Fe loading on the removal efficiency of chloroacetic acids

Fig. 6 shows the removal efficiency of chloroacetic acids with various amounts of Pd/Fe nanoparticles. It is expected that the surface area concentration of metal increased with increasing the amount of metal loading, resulting in the increase of removal efficiency of target pollutants. Arnold and Roberts found that the pseudo-first-order rate was directly proportional to metal loading over a range of 0–3.12 g/L [29]. As shown in Fig. 6, the removal efficiency of chloroacetic acids increased with increasing metal addition when metal addition was less than 3 g/L. However, the removal efficiencies were not found to increase with the increase of metal addition at Pd/Fe loading >3 g/L. This might be due to the inefficient mixing at higher metal addition and the formation of excessive hydrogen bubbles that hindered the contact between Pd/Fe nanoparticles and target pollutants [25,26,29].

3.5. Effect of initial pH value on the removal efficiency of chloroacetic acids

The requirement for H^+ participation and the generation of $O\bar{H}$ in the dechlorination of COCs indicate that the reaction rate and the extent of dechlorination may be directly influenced by pH value. Liu and Lowry reported that decreasing pH from 8.9 to 6.5 doubled the TCE dechlorination rate constant [30]. To determine the optimum pH for catalytic dechlorination of chloroacetic acid by Pd/Fe nanoparticles, the effect of pH on the removal efficiency was investigated over the range of pH 1–9. The initial pH value of the reaction system was adjusted with 0.1% sodium hydroxide solution and 0.1% sulfuric acid solution. As illustrated in Fig. 7, the removal efficiency at pH 2.98 was greater than that at other pH values. As the dechlorination is an H^+ consumption process, acidic solution facilitated the dechlorination of chloroacetic acids. An increase in initial pH value of reaction system could promote the formation of a passivating layer due to the precipitation of metal hydroxides on the surface of Pd/Fe nanoparticles [31,32].

In neutral pH or alkaline solution, Eq. (5) can occur easily, followed by the rapid oxidation of $Fe(OH)_2$ to $Fe(OH)_3$ (Eq. (6)). Consequently, the removal efficiency of chloroacetic acids decreased with increasing the pH value of the solution:

$$Fe^{2+} + OH^- \rightarrow Fe(OH)_2 \quad (5)$$

$$4Fe(OH)_2 + O_2 + 2H_2O \rightarrow 4Fe(OH)_3 \quad (6)$$

Wang et al. reported that the amount of H produced by the corrosion of Fe decreased with increasing pH value of solution,

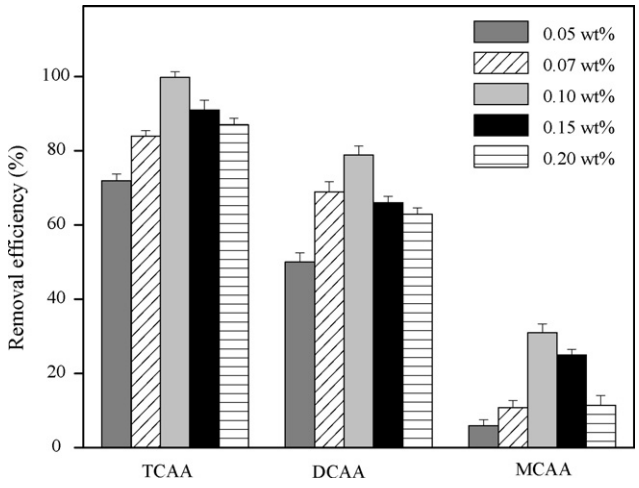

Fig. 5. Effect of Pd content on the removal efficiency of chloroacetic acids (Pd/Fe loading = 3 g/L, initial concentration of chloroacetic acids = 20 mg/L, and reaction time = 180 min). Values and the error bars represent the average and the standard deviation from the triplicate runs, respectively.

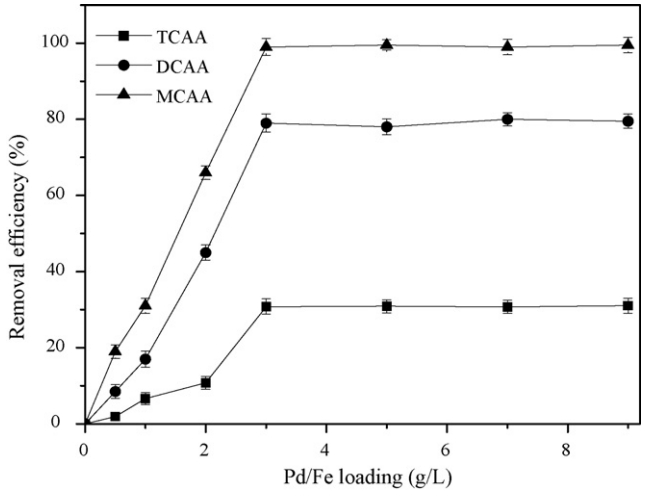

Fig. 6. Effect of Pd/Fe loading on the removal efficiency of chloroacetic acids (Pd content = 0.1 wt%, initial concentration of chloroacetic acid = 20 mg/L, and reaction time = 180 min). Error bars represent standard deviation for three measurements, and in some cases the symbols are bigger than the error bars. Each point represents the average of three measurements performed to the same sample.

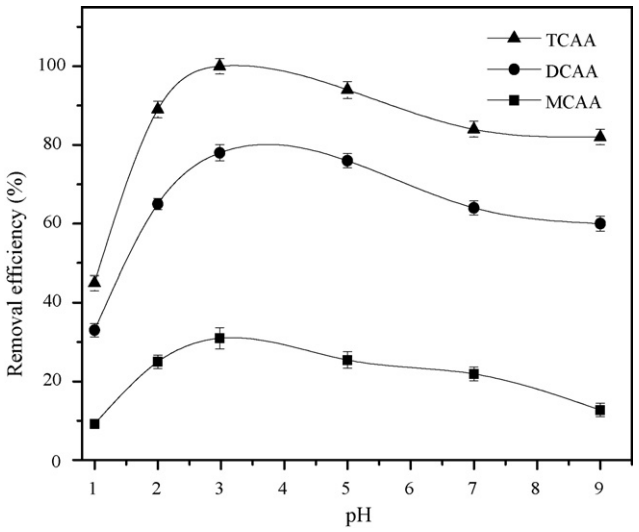

Fig. 7. Effect of initial pH value on the removal efficiency of chloroacetic acids (Pd content = 0.1 wt%, Pd/Fe loading = 3 g/L, initial concentration of chloroacetic acid = 20 mg/L, and reaction time = 180 min). Error bars represent standard deviation for three measurements, and in some cases the symbols are bigger than the error bars. Each point represents the average of three measurements performed to the same sample.

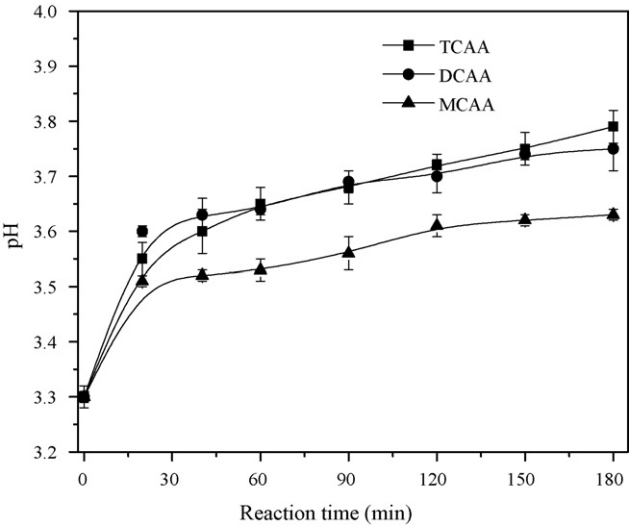

Fig. 8. Change of pH value during the removal of chloroacetic acids (Pd content = 0.1 wt%, Pd/Fe loading = 3 g/L, and initial concentration of chloroacetic acid = 20 mg/L). Error bars represent standard deviation for three measurements, and in some cases the symbols are bigger than the error bars. Each point represents the average of three measurements performed to the same sample.

resulting in the decrease of the removal efficiency of COCs [33]. Low pH condition accelerated the iron corrosion, and concomitantly increased the loss of iron base and catalyst Pd on the surface of Pd/Fe nanoparticles. The large amount of hydrogen bubbles adsorbed onto the Pd/Fe interface would inevitably deactivate Pd/Fe nanoparticles. On all accounts, no significant decrease or increase in the removal efficiency of chloroacetic acids were detected during dechlorination reaction conducted under pH

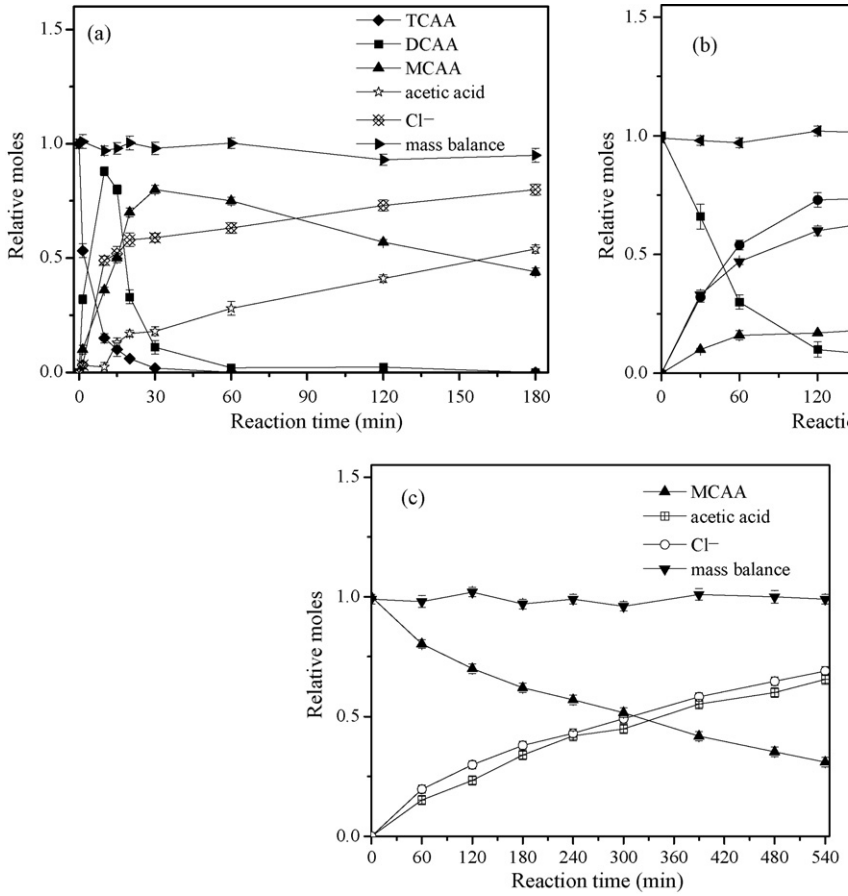

Fig. 9. Intermediates and final products of catalytic dechlorination of chloroacetic acids (Pd content = 0.1 wt%, Pd/Fe loading = 3 g/L, and initial concentration of chloroacetic acid = 20 mg/L): (a) TCAA, (b) DCAA, and (c) MCAA. Error bars in the figures represent the standard deviation between the concentrations in each of the triplicate reactors for a given treatment.

ranged from 2 to 9, indicating that the catalytic dechlorination of chloroacetic acids can be performed under wide pH range.

3.6. Change of pH during dechlorination of chloroacetic acids

The changes of pH value in the reaction system are shown in Fig. 8. The pH values measured during the dechlorination show a slight variation to basic values. The increase of pH value was probably due to the oxidation of ZVI iron. As shown in Fig. 8, the pH value increased slightly during the catalytic dechlorination of chloroacetic acid, the total increase in pH value was less than 1. This phenomenon can be explained by the consumption of H^+ with respect to the corrosion of metal iron. Interestingly, the yield of the final product of dechlorination of chloroacetic acids, acetic acid, did not result in the increasing tendency of pH value during the reaction. This phenomenon suggested that the quantity of H^+ produced in the system was very small, and the influence of the produced H^+ on the change of pH value during the dechlorination of chloroacetic acids is very limited.

3.7. Mechanism for catalytic dechlorination of chloroacetic acids

Fig. 9 illustrates the intermediates and final products formation from the catalytic dechlorination of chloroacetic acids. Along with the removal of chloroacetic acids, the chloride ions released and their concentration increased gradually. As shown in Fig. 9(a), TCAA was degraded rapidly within the first 15 min. Further, accompanied with the sequential hydrogenolysis of TCAA, MCAA and acetic acid were immediately detected in the reaction system, indicating a direct dechlorination pathway from TCAA to MCAA or acetic acid. From Fig. 9(b), the concentration of MCAA was found to increase concomitantly with the degradation of DCAA. The rapid appearance of acetic acid provided the evidence of direct conversion of DCAA to acetic acid. Compared with TCAA and DCAA, the dechlorination rate of MCAA was much slower. As can be seen from Fig. 9(c), only 59.6% MCAA was dechlorinated within 540 min.

C/C_0 versus time data were fit using a pseudo-first-order kinetic model for catalytic dechlorination of chloroacetic acids (Fig. 10). The observed reaction rate constant (k_{obs}) was calculated according to Eq. (7):

$$\ln \frac{C}{C_0} = -k_{obs} t \quad (7)$$

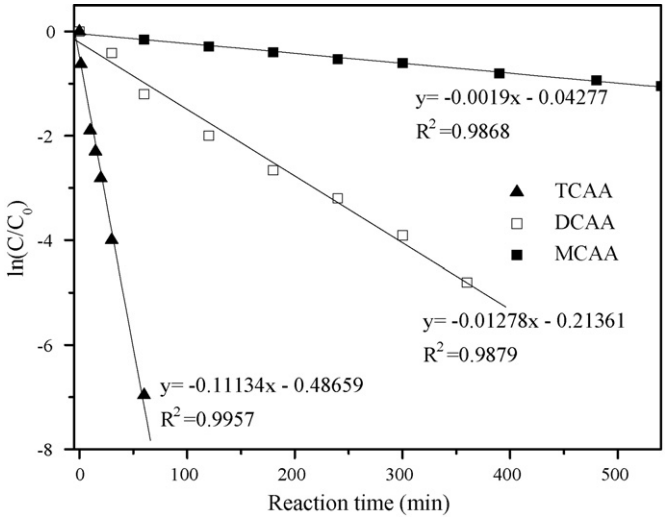

Fig. 10. Determination of the observed first-order reaction rate constant for catalytic dechlorination of chloroacetic acids.

Table 1
Observed reaction rate constants of chloroacetic acids with different metallic systems.

Chloroacetic acid	Metallic system	k_{obs}	$t_{1/2}$ (min)
TCAA	Pd/Fe nanoparticles	1.113×10^{-1}	6.228
	Fe^0 (100 mesh)[a]	9.510×10^{-3}	72.886
DCAA	Pd/Fe nanoparticles	1.278×10^{-2}	54.237
	Fe^0 (100 mesh)[a]	3.060×10^{-4}	2265.196
MCAA	Pd/Fe nanoparticles	1.900×10^{-3}	364.815
	Fe^0 (100 mesh)[a]	–	–

[a] k_{obs} of dechlorination of chloracetic acid by Fe^0 (100 mesh) was calculated based on data reported by Zhang et al. [10].

where C is the concentration of chloroacetic acid at reaction time t in aqueous phase, C_0 is initial concentration of chloroacetic acid. The values of the k_{obs} and corresponding half-lives ($t_{1/2}$) are presented in Table 1. To compare the reaction rate of dechlorination of chloroacetic acids with Fe^0 powder, the values of k_{obs} of dechlorination of TCAA and DCAA with Fe^0 (100 mesh) are also listed in Table 1. For MCAA, the dechlorination conditions of MCAA (e.g. ZVI loading and initial concentration of MCAA) were quite different from the conditions we used in this study, and the degradation of MCAA by using Fe^0 was little, the comparison was not made.

From Table 1, the catalytic dechlorination rates of chloroacetic acids by Pd/Fe nanoparticles follow the order of TCAA > DCAA > MCAA. Apparently, highly chlorinated chloroacetic acids were more readily dechlorinated than lightly chlorinated ones. This phenomenon was in good agreement with previous literature: the greater the number of chlorine substituents of chlorinated compound, the more prone the chlorinated compound to be dechlorinated [34–36]. As atomic chlorine is of high polarity, the number of substituent chlorine in molecular chloroacetic acid would influence the dechlorination efficiency. The explanation for this phenomenon is that chlorine is strongly electron withdrawing and makes the C atom of C–Cl more amenable to electrophilic attack. Thus chloroacetic acid with more chlorine atoms would be more prone to be reduced during the process of dechlorination.

4. Conclusions

A practically effective drying method, solvent replacement oven drying method, was successfully developed for drying wet Pd/Fe nanoparticles prepared by using an aqueous solution of potassium hexachloropalladate as palladizing solution:

(1) The size, shape, aggregation degree, and the catalytic dechlorination activity of dry Pd/Fe nanoparticles were significantly influenced by washing reagent used during the drying process of wet particles. Oxidation of dry Pd/Fe nanoparticles can be prevented by washing the freshly prepared Pd/Fe nanoparticles with deionized water, ethanol and acetone sequentially, followed by vacuum-dried in an oven without the protection of nitrogen. While Pd/Fe nanoparticles dried using direct oven drying method were deactivated due to the severe oxidation and aggregation.
(2) Catalytic dechlorination rates of chloroacetic acids by Pd/Fe nanoparticles in dry state follow the order of TCAA > DCAA > MCAA. Catalytic dechlorination of chloroacetic acids can be modeled as a pseudo-first-order.
(3) Accompanied with the sequential hydrogenolysis of chloroacetic acids, TCAA can be dechlorinated to DCAA, MCAA, and acetic acid directly by Pd/Fe nanoparticles. Likewise, DCAA can be catalytically dechlorinated to MCAA and acetic acid directly.

(4) Removal efficiencies of chloroacetic acids with initial concentration of 20 mg/L can be maximized at Pd content of 0.1 wt%, Pd/Fe loading of 3 g/L, and initial pH of 2.98.

Acknowledgements

This work was supported by the Program of Changjiang Scholars and Innovative Research Team in University (PCSIRT), State Key Laboratory of Urban Water Resources and Environment (No. 2008DX06), National Natural Science Foundation of China (No. 50978066), and the Training Program Foundation for Talents of Kunming University of Science and Technology (2009-036).

References

[1] P.D. Gara, E. Bucharsky, M. Wörner, A.M. Braun, D.O. Mártire, M.C. Gonzalez, Inorg. Chim. Acta 360 (2007) 1209–1216.
[2] E. Malliarou, C. Collins, N. Graham, M. Nieuwenhuijsen, Water Res. 39 (2005) 2722–2730.
[3] USEPA, Final Rule 63 (1998) 69390–69476.
[4] C.J. Clark II, P.S.C. Rao, M.D. Annable, J. Hazard. Mater. 96 (2003) 65–78.
[5] H. Song, E.R. Carraway, Appl. Catal. B 78 (2008) 53–60.
[6] G.V. Lowry, M. Reinhard, Environ. Sci. Technol. 35 (2001) 696–702.
[7] Q. Fernando, N. Korte, Environ. Sci. Technol. 31 (1997) 1074–1078.
[8] K. Venkatachalam, X. Arzuaga, N. Chopra, V.G. Gavalas, J. Xu, D. Bhattacharyya, B. Hennig, L.G. Bachas, J. Hazard. Mater. 159 (2008) 483–491.
[9] R.M. Hozalski, L. Zhang, W.A. Arnold, Environ. Sci. Technol. 35 (2001) 2258–2263.
[10] L. Zhang, W.A. Arnold, R.M. Hozalski, Environ. Sci. Technol. 38 (2004) 6881–6889.
[11] Y.X. Fang, S.R. Al-Abed, Appl. Catal. B 78 (2008) 371–380.
[12] B.H. Wang, W.B. Zhang, W. Zhang, A.S. Mujumdar, L.X. Huang, Drying Technol. 23 (2005) 7–23.
[13] G.C.C. Yang, H.L. Lee, Water Res. 39 (2005) 884–894.
[14] Y.T. He, J. Wan, T. Tokunaga, J. Nanoparticle Res. 10 (2008) 321–332.
[15] X.Y. Wang, C. Chen, Y. Chang, H.L. Liu, J. Hazard. Mater. 161 (2009) 815–823.
[16] R. Muftikian, Q. Fernando, N. Korte, Water Res. 29 (1995) 2434–2439.
[17] X.H. Xu, M.Y. Zhou, P. He, Z.W. Hao, J. Hazard. Mater. 123 (2005) 89–93.
[18] J.J. Wei, X.H. Xu, Y. Liu, D.H. Wang, Water Res. 40 (2006) 348–354.
[19] J. Morales, R. Hutcheson, I.F. Cheng, J. Hazard. Mater. 90 (2002) 97–108.
[20] W.X. Zhang, D.W. Elliott, Remediation J. 16 (2006) 7–21.
[21] F. He, D. Zhao, Environ. Sci. Technol. 41 (2007) 6216–6221.
[22] S.H. Joo, D. Zhao, Chemosphere 70 (2008) 418–425.
[23] K.T. Park, K. Klier, C.B. Wang, W.X. Zhang, J. Phys. Chem. 101 (1997) 5420–5428.
[24] P. Bodnariuk, B. Coq, G. Ferrat, F. Figueras, J. Catal. 116 (1989) 459–466.
[25] G.N. Jovanovic, P.Ž. Plazl, P. Sakrittichai, K. Al-Khaldi, Ind. Eng. Chem. Res. 44 (2005) 5099–5106.
[26] L.J. Graham, G. Jovanovic, Chem. Eng. Sci. 54 (1999) 3085–3093.
[27] F. He, D. Zhao, Appl. Catal. B 84 (2008) 533–540.
[28] H.L. Lien, W.X. Zhang, Appl. Catal. B 77 (2007) 110–116.
[29] W.A. Arnold, A.L. Roberts, Environ. Sci. Technol. 34 (2000) 1794–1850.
[30] Y.Q. Liu, G.V. Lowry, Environ. Sci. Technol. 40 (2006) 6085–6090.
[31] S.Y. Oh, D.K. Cha, P.C. Chui, Environ. Sci. Technol. 36 (2002) 2178–2184.
[32] X.H. Xu, H.Y. Zhou, D.H. Wang, Chemosphere 58 (2005) 1497–1502.
[33] J.K. Wang, J. Farrell, Environ. Sci. Technol. 37 (2003) 3891–3896.
[34] J. Feng, T.T. Lim, Chemosphere 59 (2005) 1267–1277.
[35] H.L. Lien, W.X. Zhang, J. Environ. Eng. 125 (1999) 1042–1047.
[36] H. Song, E.R. Carraway, Environ. Eng. Sci. 23 (2006) 272–284.